Scaling properties of a percolation model with long-range correlations

Muhammad Sahimi[1,2] and Sumit Mukhopadhyay[1,*]

[1]*Department of Chemical Engineering, University of Southern California, Los Angeles, California 90089-1211*
[2]*Hochstleistungsrechenzentrum, Kernforschungsanlage Jülich, D-52425 Jülich 1, Germany*
(Received 27 March 1995; revised manuscript received 17 May 1996)

We present the results of Monte Carlo simulations of a percolation model with long-range correlations in two and three dimensions. The correlations are generated by a fractional Brownian motion. The nature of the percolation transition in this model is discussed. The percolation thresholds and the critical exponents of the model are calculated. The exponents are found to be mostly *nonuniversal* and dependent on a parameter that characterizes the nature of the correlations. Some possible applications of the model are discussed in detail, including flow in *field-scale* porous media (with *megascopic* disorder) with a given permeability distribution, and estimating their effective permeability, and transport and dispersion in geological formations and explaining the anomalous and nonuniversal behavior of the dispersivity that has been observed in many field-scale experiments, in terms of the nonuniversal properties of our model. [S1063-651X(96)08109-3]

PACS number(s): 47.55.Mh, 64.60.Ak

I. INTRODUCTION

Percolation theory has become a powerful, much-used tool for investigating various phenomena in disordered media [1]. Its popularity stems from its relevance to a wide variety of phenomena [2], and from the fact that despite the simplicity of its underlying concepts, it leads to nontrivial critical phenomena. A partial list of its applications includes various flow phenomena in porous media and rock [3,4], transport, mechanical and rheological properties of disordered materials such as polymers, glasses, and powders, hopping conduction in amorphous semiconductors, frequency-dependent conductivity in superionic conductors, reaction, diffusion, and deposition in porous structures, and even earthquakes and some biological systems.

However, most percolation processes that have been studied so far deal with phenomena in which there is either no correlation, or only a short-range correlation. The nature of disorder in many important physical phenomena and media is not, however, completely random, and usually there are correlations of a given extent. For example, in packing of solid particles, whose mechanical properties are described by elastic percolation networks, there are usually some short-range correlations. However, the scaling properties of percolation with finite-range correlations are the same as those of random percolation, if the length scale of interest is larger than the correlation length. Moreover, if the correlation function decays faster than r^{-d}, where r is the distance between two points and d is the dimensionality of the system, then the critical properties of the systems are identical with those of random percolation [1]. In some other cases, e.g., field-scale porous media and aquifers, there are long-range correlations (see below), by which we mean correlations whose extent is comparable with the linear size of the system. In the past there have been a few papers that dealt with percolation with long-range correlations. The goal of this paper is to investigate various scaling properties of one such percolation model, recently introduced by one of us [5], and point out its possible applications. But, let us first summarize the most important scaling properties of percolation networks that we wish to study in this paper.

Consider a two- or three-dimensional percolation network in which a fraction p of the bonds are conducting (we refer to such bonds as the open bonds), and the rest are insulating (their conductance is zero). Near the percolation threshold p_c one can define a correlation length ξ_p which diverges as p_c is approached according to the power law $\xi_p \sim (p - p_c)^{-\nu}$. The correlation length is the length scale for macroscopic homogeneity of the system. For any length scale $L \gg \xi_p$ the system is macroscopically homogeneous, while for length scales $L \ll \xi_p$ the system is a fractal and statistically self-similar object. Near p_c the accessible fraction X^A of conducting bonds, i.e., those that are in the sample-spanning cluster, vanishes as $X^A \sim (p - p_c)^\beta$. For any length scale $L \ll \xi_p$ the sample-spanning cluster is a fractal object with a fractal dimension $D_p = d - \beta/\nu$ for a d-dimensional system. The sample-spanning cluster can be divided into two parts: the dead-end part that carries no flow or current, and the *backbone*, which is the multiply connected part of the cluster. Near p_c the fraction X^B of the conducting bonds that are in the backbone vanishes as $X^B \sim (p - p_c)^{\beta_B}$, while for any length scale $L \ll \xi_p$ the backbone is a fractal object with a fractal dimension $D_B = d - \beta_B/\nu$. Similarly, the overall conductivity G of the network vanishes as p_c is approached according to the power law $G \sim (p - p_c)^t$. If the open bonds of the network represent the pores or channels of a porous medium through which a fluid can flow, a hydrodynamic permeability K can be defined that near p_c obeys the scaling law

$$K \sim (p - p_c)^e. \tag{1}$$

Currently accepted values of these critical exponents are $\nu = \frac{4}{3}$ and 0.88, $\beta = \frac{5}{36}$ and 0.41, $\beta_B \simeq 0.48$ and 0.99, $D_p = \frac{91}{48}$ and 2.52, and $D_B \simeq 1.64$ and 1.87 for $d = 2$ and 3, respectively.

*Present address: Applied Mathematics Research Center, Mathematical Sciences Building 1395, Purdue University, West Lafayette, IN 47907-1395.

For most conductance and permeability distributions one has $t=e\simeq1.3$ and 2 for $d=2$ and 3, respectively. However, there are certain cases for which $t\neq e$. Throughout this paper we treat e as a distinct exponent.

The plan of this paper is as follows. In the next section we describe the percolation model that we study in this paper. We then present and discuss the results of extensive Monte Carlo simulations of the model. The paper is summarized in the last section, where we discuss possible applications of the model.

II. PERCOLATION WITH LONG-RANGE CORRELATIONS

One of the first studies of correlated percolation was carried out by Coniglio et al. [6]. However, the range of correlations in their model was finite. The first model of percolation with long-range correlations was probably proposed by Weinrib and Halperin [7] and Weinrib [8]. In their model, a site percolation problem was defined by site-occupation variables s_i at the sites $\{i\}$ of a regular lattice of dimensionality d, which take on the values 1 and 0 corresponding to occupied and vacant sites, respectively. For the corresponding bond percolation problem, the $\{i\}$ label bonds. The system is characterized by the site-occupation probability

$$p=\langle s_i\rangle, \tag{2}$$

and the site-occupation correlation function

$$C(|\mathbf{r}_i-\mathbf{r}_j|)=\langle s_i s_j\rangle-\langle s_i\rangle\langle s_j\rangle, \tag{3}$$

where $\langle\ \rangle$ is an average over all realizations of the random variables $\{s_i\}$. For a statistically isotropic system, the correlation function depends only on the distance $|\mathbf{r}_i-\mathbf{r}_j|$ between two sites at positions $\mathbf{r}_i$ and $\mathbf{r}_j$. For example, for random percolation $C(r)=p(1-p)\delta_{r,0}$. Weinrib and Halperin [7] and Weinrib [8] considered the case for which

$$C(r)\sim r^{-\lambda}, \tag{4}$$

where $\lambda<d$. For $\lambda\geq d$, the critical properties of the system are identical with those of random percolation, and thus are not of interest to us. Weinrib [8] showed that for $\lambda<d$

$$\nu=\frac{2}{\lambda}. \tag{5}$$

Other critical exponents of this percolation model were also calculated to linear order in terms of $\epsilon=6-d$ and $\delta=4-\lambda$. Isichenko and Kalda [9] argued that for $2/\nu>\lambda>0$ the critical exponent β should be the same as that of random percolation. However, this does not agree with field-theoretic results of Weinrib [8].

Prakash et al. [10] considered a slightly different percolation model in which the correlation function $C(r)$, defined by

$$C(r)=\langle u(r')u(r+r')\rangle, \tag{6}$$

where $u(r)$ is a random variable obeying the distribution with long-range correlations, and denotes an average over all values of r', in a d-dimensional system is given by

$$C(r)\sim r^{-(d-\zeta)}, \tag{7}$$

where $-2\leq\zeta\leq2$ is a parameter of their model, such that $0\leq\zeta\leq2$ represents positive correlations, while $-2\leq\zeta\leq0$ corresponds to negative correlations. Prakash et al. [10] studied this model in two dimensions (2D) and showed that for $\zeta\leq0.5$ there is no change in ν from the uncorrelated value $\nu=\frac{4}{3}$. For $0.5\leq\zeta\leq1.0$ their results were consistent with Weinrib's results [8] [see Eq. (5)]

$$\nu=\frac{2}{d-\zeta}, \tag{8}$$

but for $\zeta\geq1.0$ their estimated ν's were consistently lower than the predictions of Eq. (5). Moreover, the fractal dimension D_p of the sample-spanning cluster was found to be unaltered by the correlations. Schmittbuhl, Vilotte, and Roux [11] studied simple models of percolation with long-range correlations using self-affine surfaces.

We now describe our percolation model with long-range correlations. Consider a stochastic process $B_H(\mathbf{r})$, called fractional Brownian motion (fBm) [12], with the following properties:

$$\langle B_H(\mathbf{r})-B_H(\mathbf{r}_0)\rangle=0, \tag{9}$$

$$\langle[B_H(\mathbf{r})-B_H(\mathbf{r}_0)]^2\rangle\sim|\mathbf{r}-\mathbf{r}_0|^{2H}, \tag{10}$$

where $\mathbf{r}=(x,y,z)$ and $\mathbf{r}_0=(x_0,y_0,z_0)$ are two arbitrary points, and H is called the Hurst exponent. A remarkable property of fBm is that it generates correlations whose extent is *infinite*. For example, consider the one-dimensional case and define an incremental correlation function $C_i(x)$ of the "future" increments $B_H(x)$ with the "past" increments $B_H(-x)$ by (the meaning of past and future becomes clear if we replace x with a time variable)

$$C_i(x)=\frac{\langle-B_H(-x)B_H(x)\rangle}{\langle B_H(x)^2\rangle}, \tag{11}$$

then one finds that $C_i(x)=2^{2H-1}-1$, *independent* of r. Moreover, the type of correlations can be tuned by varying H. If $H>\frac{1}{2}$, then $C_i(x)>0$ and fBm displays *persistence*, i.e., a trend (for example, a high or low value) at x is likely to be followed by a similar trend at $x+\Delta x$. If $H<\frac{1}{2}$, then $C_i(x)<0$ and fBm generates *antipersistence*, i.e., a trend at x is not likely to be followed by a similar trend at $x+\Delta x$. For $H=\frac{1}{2}$ the *trace* of fBm is similar to that of a random walk, and the *increments* are uncorrelated. For $H=-\frac{1}{2}$ the process is equivalent to a *white noise* and is completely random. Fractional Brownian motion has found many applications.

A convenient way of representing a distribution function is through its spectral density $S(\boldsymbol{\omega})$, the Fourier transform of its variance. For example, for a d-dimensional fBm it can be shown that

$$S(\boldsymbol{\omega})\sim\frac{1}{(\Sigma_{i=1}^d\omega_i^2)^{H+d/2}}, \tag{12}$$

where $\boldsymbol{\omega}=(\omega_1,...,\omega_d)$. This spectral representation also allows us to introduce a cutoff length scale $\ell_{co}=1/\sqrt{f_{co}}$ such that

$$S(\boldsymbol{\omega}, f_{co}) \sim \frac{1}{(f_{co} + \Sigma_{i=1}^{d} \omega_i^2)^{H+d/2}}. \quad (13)$$

This cutoff length scale allows us to control the scale over which the spatial properties of a system are correlated (or anticorrelated). Hence for length scales $\ell < \ell_{co}$ they preserve their correlations (anticorrelations), but for $\ell > \ell_{co}$ they become random and uncorrelated. In d dimensions, the limit $H = -d/2$ represents a white-noise process which is completely random. The spectral density representation also provides a convenient method for generating a sequence of numbers that obey a distribution with long-range correlations, using a fast Fourier transform technique. For example, in the case of fBm, one first generates random numbers, uniformly distributed in (0,1), and assigns them to the sites or bonds of a d-dimensional network. The Fourier transform of the resulting d-dimensional array of the numbers is then calculated numerically. The Fourier-transformed numbers are then multiplied by $\sqrt{S(\boldsymbol{\omega})}$, and the results are then inverse Fourier transformed back into the real space. The numbers so obtained obey a spatial distribution with the desired long-range correlations. To avoid the problem associated with the periodicity of the numbers arising as a result of their Fourier transforming, one has to generate the array for a much larger network than the actual size that is to be used in the simulations, and use the central part of the network. In the discussion of our results, when we refer to the size of a network, we mean the size of its central part that we used in our percolation simulations. An alternative algorithm for simulating fBm, based on its integral representation, is described by Rambaldi and Pinazza [13]. The spectral representation of distribution functions has been discussed in detail by Hardy and Beier [14].

A fBm was used by Sahimi [5] for generating a percolation model with long-range correlations. The motivation for his work was provided by the work of Hewett and Behrens [15,16], who analyzed the permeability distributions and porosity logs of heterogeneous rock formations at large length scales (of order of hundreds of meters). He argued that the porosity distribution follows a fractional Gaussian noise (fGn), whose spectral density in, e.g., 1D, is given by

$$S(\omega) \sim \frac{1}{\omega^{2H-1}}. \quad (14)$$

It can be shown that fGn corresponds, roughly speaking, to the derivative of fBm. Vertical porosity logs analyzed by Hewett [15] produced values $H > 0.5$, indicating the existence of long-range positive correlations. The exponent H, so obtained, was subsequently used for generating areal heterogeneity maps by simulating fBm statistics.

We have reanalyzed [17] Hewett's data, as well as extensive porosity and permeability data from several oil fields in southwest Iran. By using various methods of analyzing the data, such as the standard rescaled-range (R/S) method, the covariance technique, and wavelet analysis, we have reached the following conclusions. (1) The porosity data do indeed show long-range correlations, as found by Hewett and others, and can be well represented by a fBm. However, unlike the findings of most of the previous authors [14–16] who found that $H > 0.5$, i.e., positive long-range correlations, we

have found that $0 < H < 0.3$, indicating negative long-range correlations. We have shown that [17–19] the reason for the difference between our results and those of the previous authors is that the standard (R/S) method that was used in most of the previous studies is fundamentally biased and unreliable. By generating *synthetic* correlated data over a wide range of H, we have shown [19] that the (R/S) method *always* predicts $0.7 < H < 0.9$, *regardless* of the value of H used for generating the data. (2) We have found that the permeability data may be represented approximately by fBm with $H < 0.2$. In a recent paper Neuman [20] has reached a similar conclusion. Some of our data yielded a *negative* value of H, indicating a trend towards the white-noise limit and complete randomness. Some authors have argued that the permeability K and porosity ϕ are related exponentially. For example, Hinrichsen *et al.* [21] used the following relation between the permeability and porosity:

$$K = 10^{a\phi + b}, \quad (15)$$

where a and b are parameters that they varied in a range that could highlight contrast in the local permeability distribution. While Eq. (15) has been used in some field-scale simulation of flow problems, we have not found any indication for its validity in our own data. One reason for this could be that Iranian oil fields are mostly carbonate reservoirs, which are fundamentally different from the sandstone reservoirs studied so far. Moreover, there cannot be a general relation, such as Eq. (15), between K and ϕ, since obviously one can have many porous media with the same porosity but vastly different permeabilities. In any event, even if we use a fGn or fBm to generate a correlated porosity field, and then employ an equation such as (15) to generate the corresponding permeability field, the resulting permeability field would contain long-range correlations, and while its properties would not be similar to one that is generated directly by a fGn or fBm, for every H used in generating the porosity field we would have a corresponding permeability field which would contain the main ingredient of our model, namely, the long-range correlations. Thus, based on our own data, we have used fBm for directly generating a permeability field with long-range correlations.

Before we describe our correlated percolation model, we point out that a fBm is *not* a stationary stochastic process, and as a result its correlation function, defined by Eq. (6), depends on *both* r and r', and not just $|r - r'|$ alone. This distinguishes our correlated percolation model from the previous models. Our correlated percolation model is as follows [5]. We first generate a correlated permeability field by assigning to each bond of a network a number selected from a fBm. To construct a percolation network and to preserve the correlations between the bonds, we remove those bonds that have been assigned the *smallest* (or the largest) permeabilities. The idea is that in rock with a broad distribution of the permeabilities, a finite volume fraction of the rock should have a small permeability, and therefore its contribution to the overall permeability of the system would be small. Alternatively, the removed bonds can be interpreted as the regions that have been plugged as the result of a phenomenon such as precipitation of solid particles on the surface of their pores. Such a precipitation process is the result of migration
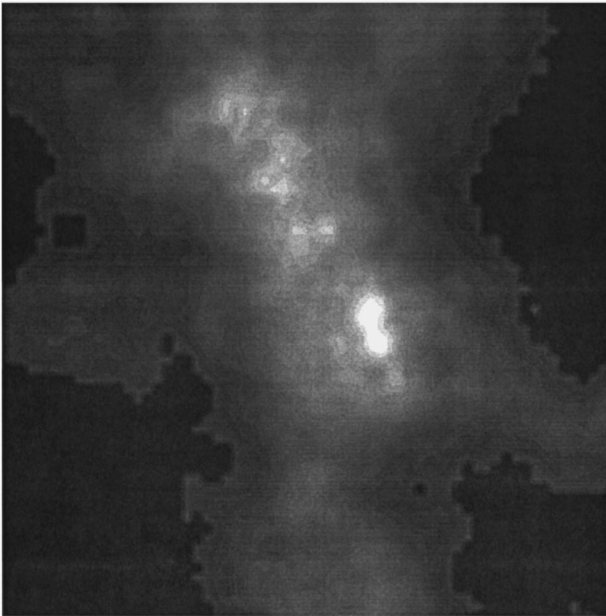
FIG. 1. A correlated percolation cluster with $H=0.8$ in which 30% of the bonds with the lowest permeabilities have been removed. Lightest and darkest areas correspond to the regions with the highest and lowest permeabilities, respectively.

of fines (small, electrically charged particles) that occurs during water flooding that is used for increasing oil production from underground reservoirs [22]. Figure 1 shows a square network in which the permeabilities have been selected according to a fBm with $H=0.8$, and 30% of its bonds with the smallest permeabilities have been removed, whereas Fig. 2 shows the same network in which the same fraction of the bonds have been removed *at random*. The striking difference between the two is due to the positive correlations induced by the fBm, as a result of which most bonds with large or
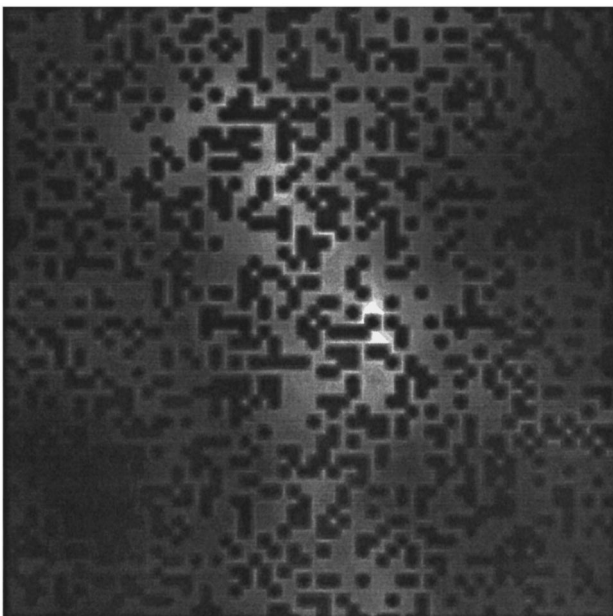
FIG. 2. The same as in Fig. 1, but in which 30% of the bonds have been removed *at random*.
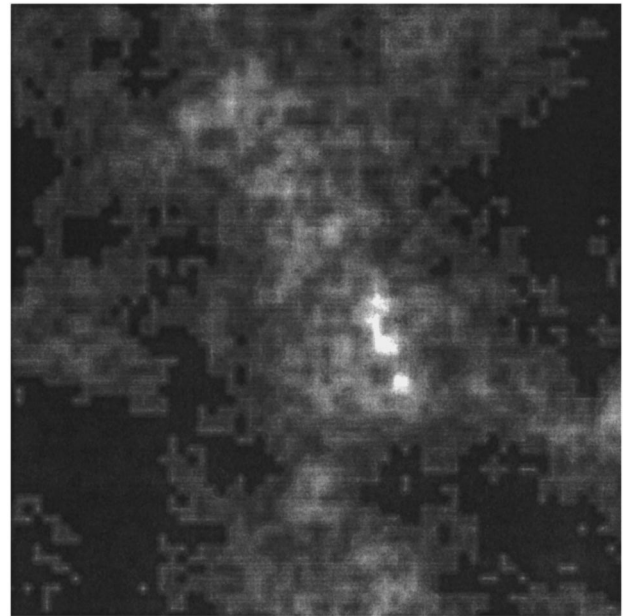

FIG. 3. A correlated percolation cluster with $H=0.2$ in which 30% of the bonds with the lowest permeabilities have been removed.

small permeabilities are clustered together. Moreover, as we can see in Fig. 1, the sample-spanning cluster generated by this model for $H>\frac{1}{2}$ does not have many dead-end bonds and is close to its backbone. This assertion is confirmed by the numerical results discussed below. Figure 3 shows a square network in which the permeabilities are distributed according to a fBm with $H=0.2$, with 30% of the bonds with the smallest permeabilities removed.

To demonstrate the broadness of the permeability distribution that is generated by a fBm, we present in Fig. 4 the normalized frequency distribution of the permeabilities generated by a 2D fBm on a square network. As this figure indicates, the distribution becomes broader with increasing H. For $H=0.7$, the permeabilities vary by more than two orders of magnitude, while for $H=0.3$ they vary over more than one order of magnitude.
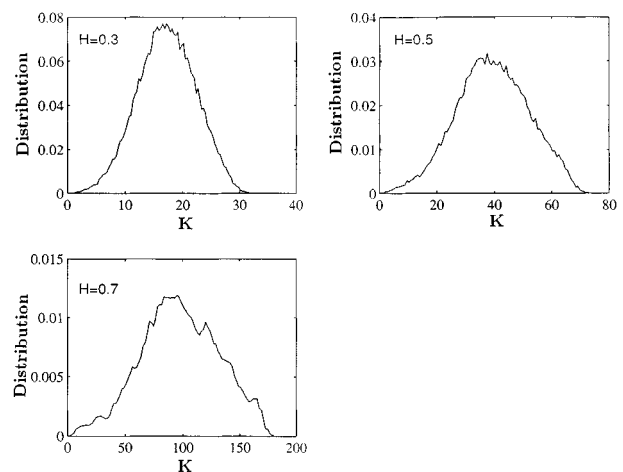

FIG. 4. The permeability distributions that are generated by a 2D fBm for three values of the parameter H.
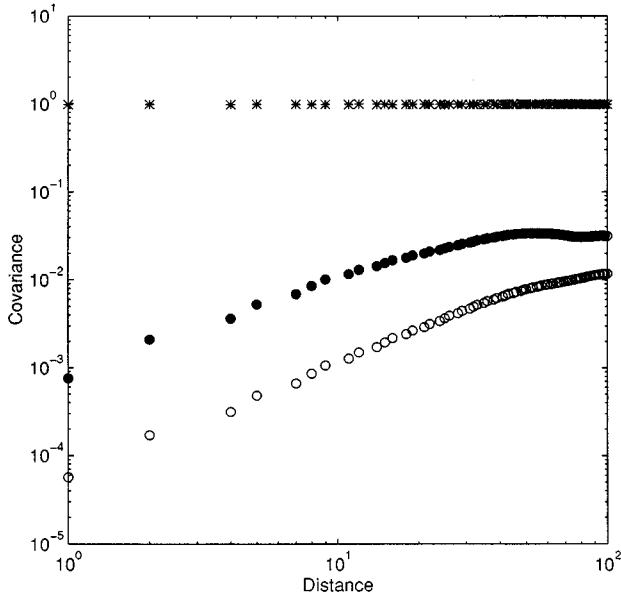
FIG. 5. The correlation function $C(r)$ on a square network in which the bond permeabilities are distributed according to a fBm. The results are, from top to bottom, for the crossover variable $f_{co}=1$, 10^{-4}, and 0.

To show that, despite the finite size of the networks that we use in our simulations, the generated permeability fields preserve the correlations, we present in Fig. 5 the covariance $V(r)$ of the fBm. The results are for a 256×256 square network (the largest 2D size used in our studies), $H=0.7$, and three values of the cutoff f_{co}. As can be seen, when $f_{co}=1$, i.e., when the length scale $\ell_{co} = 1\sqrt{f_{co}}$ over which the permeabilities are correlated is small (all lengths are measured in units of a network bond), the covariance function is essentially constant, since the system is almost completely random. For $f_{co}=10^{-4}$ the covariance function becomes a constant beyond $r = \ell_{co} = 10^2$, whereas for $f_{co}=0$, i.e., when $\ell_{co} = \infty$ and the permeabilities are correlated at all length scales, the covariance is never a constant. In fact, since for fBm [see Eq. (10)] $V(r) \sim r^{2H}$, the covariance increases with $H>0$ and r, and the results shown in Fig. 5 confirm this. This demonstrates that the finite size of the networks used in our simulations is large enough and does not distort or destroy the properties of fBm.

We have studied various scaling properties of this percolation model, and have calculated the relevant critical exponents discussed above. In particular, we have studied this percolation model in the square and simple-cubic networks, and have calculated p_c, ν, β_B, D_p, D_B, and e for the entire range $-\frac{1}{2} \leq H < 1$. We have found that, as H approaches $-\frac{1}{2}$ the white-noise limit in 1D, the critical exponents already approach their value for random percolation. Thus negative values of H essentially generate distributions that are more or less random. To calculate the percolation threshold p_c, we used networks of various linear size L, and for each L we calculated the *effective* percolation threshold $p_c(L)$ at which a given quantity, such as the backbone fraction X^B, vanishes. The results were then averaged over a large number of realizations, ranging from a few thousand for small values of L to 100 for the largest values of L. Except for calculating the correlation function shown in Fig. 5, the largest network

sizes that we used, after deleting the boundary regions of network to avoid the problems with periodicity of the Fourier-transformed array of numbers (see above), were $L=256$ and 64 in 2D and 3D, respectively. According to finite-size scaling theory [23–25]

$$p_c(L) - p_c \sim L^{-1/\nu}, \tag{16}$$

so that a fit of the results for $p_c(L)$ to Eq. (16) yields both p_c and ν.

To estimate the permeability exponent e, we first calculated the permeability of the networks by applying a unit pressure gradient to them, and assuming that each bond represents a region of the pore space through which fluid flow occurs, whose permeability was selected from a fBm described above. Assuming a uniform cross-sectional area for the bonds, and writing a mass balance for a node i of the network, $\Sigma_j Q_{ij}=0$, yields a set of simultaneous equations for the nodal pressures. Here $Q_{ij}=k_{ij}\Delta P_{ij}$, where k_{ij} is the permeability of bond ij and ΔP_{ij} the pressure drop along it. We used periodic boundary conditions in the direction(s) perpendicular to the direction of the pressure gradient. This set of equations was solved by a successive over-relaxation method in 2D and a conjugate gradient method in 3D. From the solution of this set, the effective permeability of the network was calculated, and the result was averaged over many realizations of the network. Although there are some efficient algorithms for identifying the sample-spanning cluster and its backbone [26], we used the solution to the pressure equations to also identify the backbone by finding the dead-end bonds of the network—those along which the pressure drop was smaller than a small number (of the order of 10^{-4})—and removing them from the sample-spanning cluster. The remaining bonds constitute the backbone of the network. In this way, the backbone fraction X^B was calculated for a given p, the fraction of permeable bonds of the network. The critical exponent e of the permeability can be calculated from the finite-size scaling theory [23,24], according to which at the percolation threshold

$$K(L, p_c) \sim L^{-e/\nu}, \tag{17}$$

while the backbone fraction obeys the scaling law

$$X^B \sim L^{-\beta_B/\nu}, \tag{18}$$

and the backbone fractal dimension is calculated by noting that at p_c the number of bonds N_B in the backbone is given by

$$N_B \sim L^{D_B}. \tag{19}$$

As is well known, if L is relatively small, one has to include the correction-to-scaling terms in Eqs. (16)–(18), in order to obtain accurate estimates of the exponents. For example, Eq. (17) should be rewritten as $K(L, p_c) \sim L^{-e/\nu}[a_1 + a_2 f_1(L) + a_3 f_2(L)]$, where $f_1(L)$ and $f_2(L)$ are the correction-to-scaling functions, and the a's are constant. This method does require a precise estimate of p_c. However, because of the large network sizes that we used, we found such corrections to be small. Alternatively, one can plot $\log[K(p)]$ versus $\log(p - p_c)$ for p close to p_c, with the slope of the resulting straight line being e. A similar method
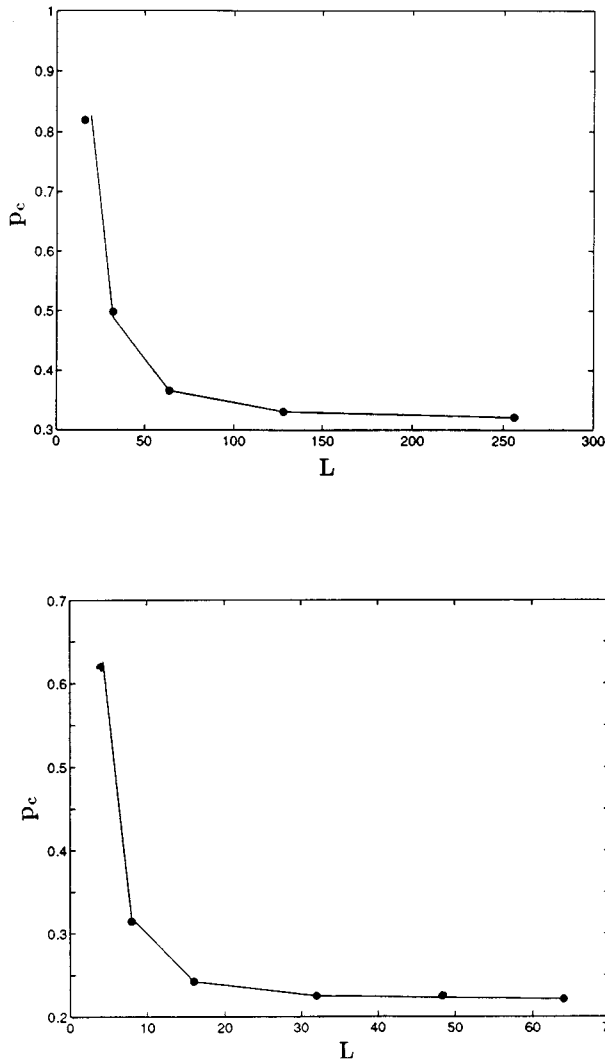
FIG. 6. The dependence of the effective percolation threshold $p_c(L)$ on the linear size L of the square network (top) and the simple-cubic network (bottom). The curves are a guide to the eye.

can be used for estimating β_B. If accurate data are obtained, and if large values of L are used, the two methods yield essentially identical results. We used both methods in order to check the accuracy of our results. Moreover, using the same methods, we carried out extensive simulations in the limit in which all the long-range correlations vanish and our percolation model becomes equivalent to random percolation. The agreement between our results in this limit and those of random percolation confirms the accuracy of our method (see below).

III. RESULTS AND DISCUSSION

The first issue we discuss is the effect on our results of the finite size of the networks used in our simulations since, strictly speaking, all the scaling laws of percolation are valid only for infinitely large networks. Although we already showed that the finite size of the networks does not destroy the correlations (see Fig. 5), we also studied how the effective values of $p_c(L)$ vary with L. This can tell us what linear size L approximates an ''infinite'' network. In Fig. 6 we

show the dependence of $p_c(L)$ of the square and simple-cubic networks on their linear size L. As can be seen, as L increases the effective values of $p_c(L)$ decrease sharply. However, beyond a minimum size L_m there is only a very weak dependence of p_c on L, if any. This minimum size is about $L_m=150$ for the square network and $L_m=30$ for the simple-cubic network. We conclude that if the percolation and permeability properties of our networks are calculated with sizes $L>L_m$, the results will be independent of L. Since most of our calculations discussed below are for $L=256$ (the square network) and $L=64$ (the simple-cubic network), we are confident that our results are not affected by finite-size effects.

In general, we find that correlations (positive or negative) change the percolation threshold of the system from its value for random percolation. However, the direction of the change depends on whether we progressively remove the highest or the lowest permeable bonds from the network. This can be seen in Fig. 7 where we present the results for various values of H. These results were obtained by progressively removing the bonds with the *lowest* permeabilities. Had we removed the bonds with the *highest* permeabilities, the percolation threshold p_{ch} of the resulting network would be just $p_{ch}=1-p_{cl}$ (see below), where p_{cl} is the percolation threshold shown in Fig. 7. This figure shows that, as H increases from its value for the random case, $H=-\frac{1}{2}$, the percolation threshold p_{cl} of the system decreases from its corresponding values for random percolation which are $p_c=\frac{1}{2}$ and 0.2488 for the square and simple-cubic network, respectively. The reason for this is that the low or high permeable regions are clustered together, so that if, e.g., we remove the bonds with the lowest permeabilities, clustering of the high-permeability bonds still generates a sample-spanning cluster, even if the fraction of the removed bonds is below the percolation threshold of the network in random percolation. Figure 7 also indicates that only when $H=-\frac{1}{2}$ do our results approach those for random percolation, so that although the incremental correlation function defined by Eq. (11) vanishes at $H=\frac{1}{2}$, the percolation properties of our model become identical with those of random percolation only at $H=-\frac{1}{2}$.

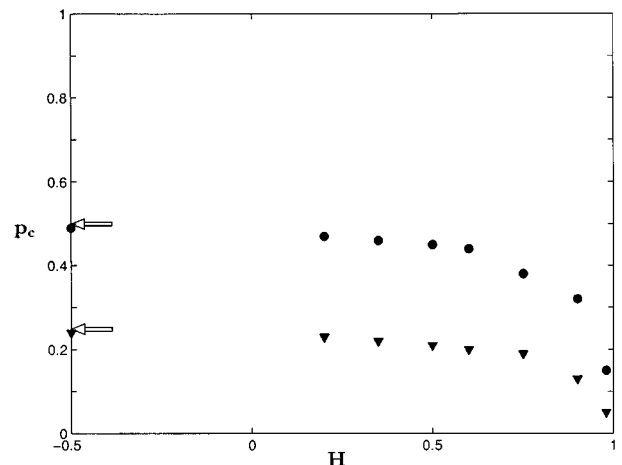What is the nature of percolation transition in our model?

FIG. 7. The dependence of the bond percolation threshold p_c of the square (circles) and the simple-cubic (triangles) networks on H. Arrows indicate the corresponding values for random percolation.
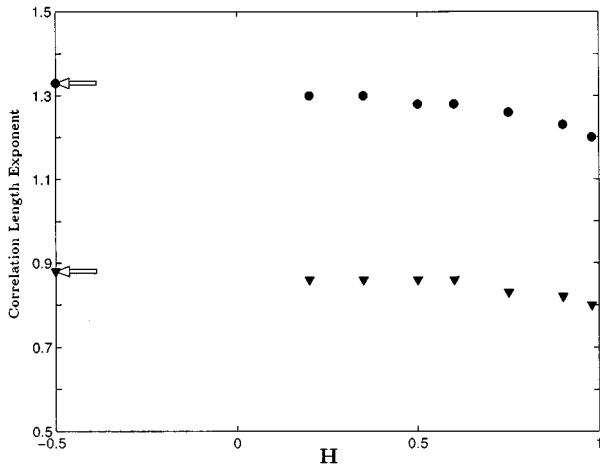
FIG. 8. The dependence of the correlation length exponent ν on H in 2D (circles) and 3D (triangles). Arrows indicate the corresponding values for random percolation.
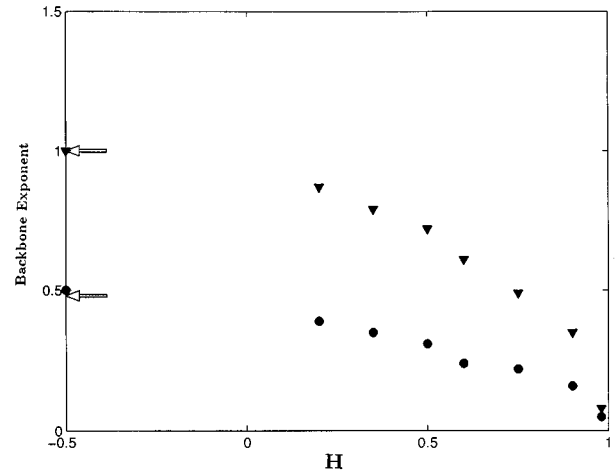

FIG. 9. The dependence of the backbone exponent β_B on H in 2D (circles) and 3D (triangles). Arrows indicate the corresponding values for random percolation.

To answer this question we also calculated a few geometrical exponents of our model. We found that ν depends weakly on H; this can be seen in Fig. 8, where we show the dependence of ν on H. In 2D, our initial simulations [5] indicated that D_p may retain its value for random percolation, $D_p = \frac{91}{48} \simeq 1.9$. However, estimating D_p accurately in 2D proved to be difficult. The sample-spanning correlated percolation cluster appears to be compact, even at p_c. Since for random percolation in 2D $D_p \simeq 1.9$ is only slightly less than 2, the Euclidean dimension, it is difficult to distinguish $D_p \simeq 1.9$ from $D_p = 2$. The matter becomes clear only in 3D where our calculations indicate that at least for $H > 0.5$ the sample-spanning cluster at p_c is nearly compact, and in fact $D_p \to 3$ as $H \to 1$. For $0 < H < 0.5$ the sample-spanning cluster at p_c is less compact, although it still appears to be very dense. Only when $H \to -\frac{1}{2}$ does D_p approach its value for random percolation, $D_p \simeq 2.52$. Since $D_p = d - \beta/\nu$, the fact that $D_p \simeq d$ for $0 < H < 1$ means that the critical exponent β is essentially zero. A zero value of β may indicate that the percolation transition *on the sample-spanning cluster* is first order, in contrast with random percolation, for which the transition is second order. However, as our results for the backbone (see below) indicate, the percolation transition on the backbone is second order. Thus, unlike the random percolation, there is a distinct difference between the nature of the percolation transition on the sample-spanning cluster and its backbone, if there are long-range correlations of the type that exist in our model. Note, however, that the hull of the sample-spanning cluster, i.e., its external surface or perimeter, is very rough, and is probably fractal with a well-defined fractal dimension, which may then indicate that the percolation transition on the hull of the clusters is also second order. Thus our percolation model offers a rich and intriguing variety of possibilities that do not exist in the random percolation.

These results can be understood better if we study the properties of the backbone of the correlated percolation cluster. Figure 9 presents the dependence of the backbone exponent β_B on H for $d = 2$ and 3, while Fig. 10 shows variations of the fractal dimension D_B with H, thus confirming that the percolation transition on the backbone of our model is second order. We also found that D_B increases with H, that

$D_B \to d$ as $H \to 1$, and that for $H > \frac{1}{2}$ the sample-spanning cluster and its backbone are similar. Since $D_p > D_B$, the results shown in Fig. 10 confirm the near compactness of the sample-spanning cluster at p_c. However, for $H < 0$ the difference between D_p and D_B increases, as they approach their values for random percolation in the limit $H = -\frac{1}{2}$, $D_p \simeq 2.52$ and $D_B \simeq 1.87$.

Figure 11 compares the permeability of a correlated square network with that of a random one. These results were obtained for $H = 0.8$. As can be seen, the permeabilities of the two networks are drastically different. Similar results were obtained for the simple-cubic network. On the other hand, if we compare the permeability of a correlated network with $H < \frac{1}{2}$ with that of a random network, the difference between the two is not as drastic as that shown in Fig. 11. This is clearly seen in Fig. 12 where we compare the results for a simple-cubic network with $H = 0.2$. These results indicate that, if $H < \frac{1}{2}$ and the fraction of the removed bonds is not too large, the difference between the permeability of a correlated network and that of a random one is relatively
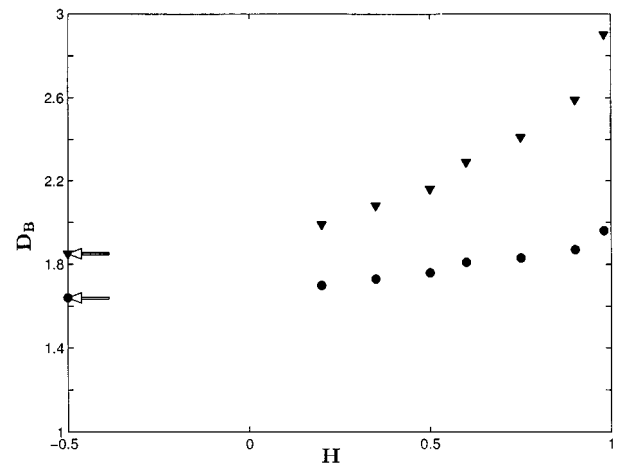

FIG. 10. The dependence of the fractal dimension D_B of the backbone on H in 2D (circles) and 3D (triangles). Arrows indicate the corresponding values for random percolation.
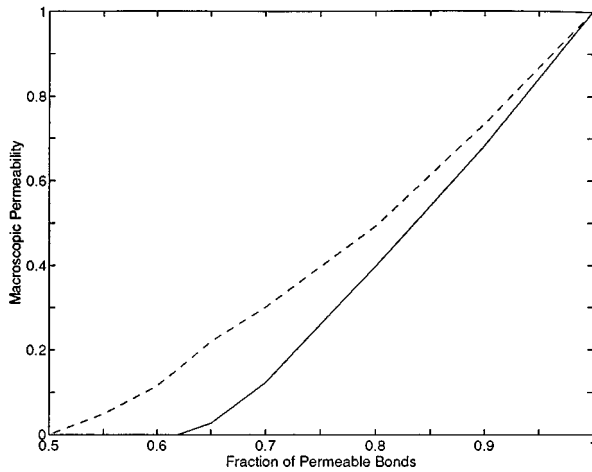
FIG. 11. The permeability of a correlated square network (solid curve) with $H=0.8$, and its comparison with that of a random square network. In the correlated network the bonds with the *highest* permeabilities are progressively removed until the percolation threshold is reached.

small. Only when the percolation threshold is approached does the difference become large. This is due to the negative nature of the correlations for $H<\frac{1}{2}$. In this regime, the clustering of the high- or low-permeability bonds does not occur very easily, and as a result with decreasing H the distribution of the permeabilities of the bonds becomes increasingly random as H approaches $-\frac{1}{2}$.

Figure 13 shows the logarithmic plot of the permeability of a 256×256 correlated square network versus $p-p_c$ near the percolation threshold for $H=0.9$. This figure shows that, similar to random percolation, near p_c the permeability does follow Eq. (1), confirming again that the percolation transition on the backbone of our model is second order. Since for $H>\frac{1}{2}$ one has positive correlations, high- or low-permeability bonds cluster together, and as a result sample-to-sample fluctuation of the permeability is not large. This means that, as discussed above, the critical exponent e of the permeability can be accurately estimated from plots such as that shown in Fig. 13. However, we also found that the same is true for
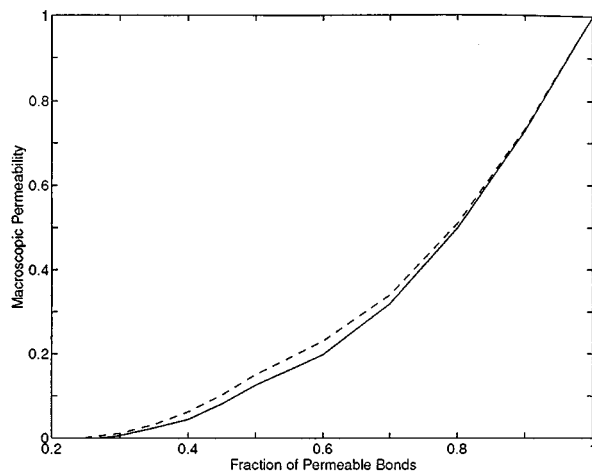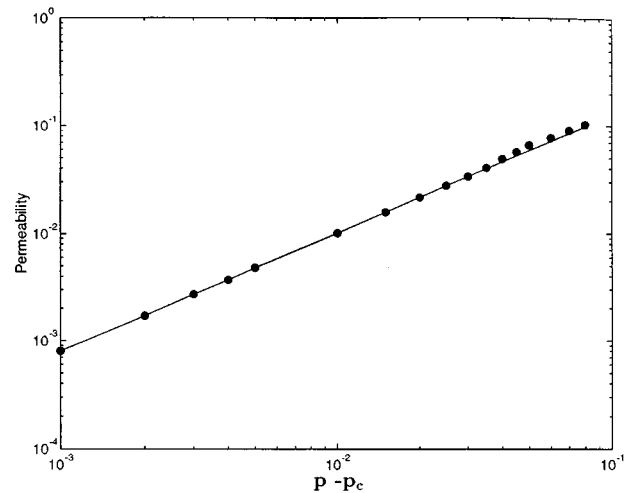

FIG. 13. Logarithmic plot of the permeability K of a 256×256 correlated square network with $H=0.9$, vs $p-p_c$. The straight line is a guide to the eye.

$H<\frac{1}{2}$. An example is shown in Fig. 14, where we show the logarithmic plot of the permeability of a 64×64×64 correlated simple-cubic network versus $p-p_c$ for $H=0.35$. Similar to Fig. 13, Eq. (1) is completely obeyed and no significant deviation from it is observed. To check the accuracy of the critical exponent e estimated from figures such as 13 and 14, we also estimated them by finite-size scaling discussed above, which is believed to be the most accurate method of estimating a critical exponent, if a precise estimate of p_c is available. The results obtained by this method agreed completely with those obtained from figures such as 13 and 14. Figure 15 shows the estimates of the critical exponent e and its dependence on H. Unlike random percolation for which the exponent e is largely universal (except for some special cases [27]), for our correlated percolation model the exponent e depends smoothly on H. This is similar to the results of Prakash *et al.* [10], who found that the critical exponent t of the conductivity of their model depends on the parameter ζ (see above). The implication of this nonuniversal behavior of e is discussed below.
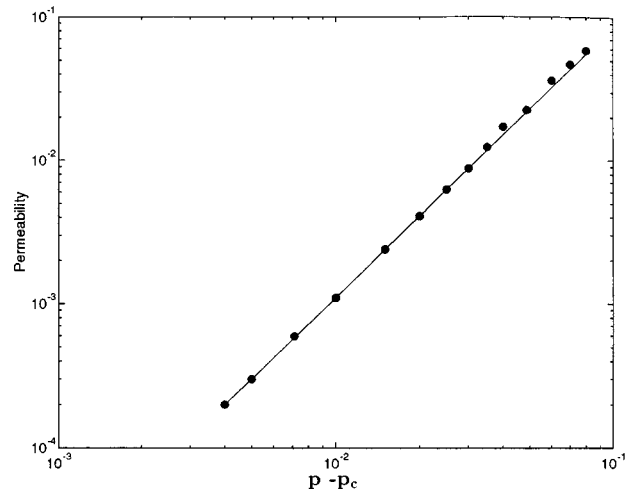

FIG. 12. The same as in Fig. 11, but for a simple-cubic network with $H=0.2$.

FIG. 14. The same as in Fig. 13, but for a 64×64×64 simple-cubic network with $H=0.35$.
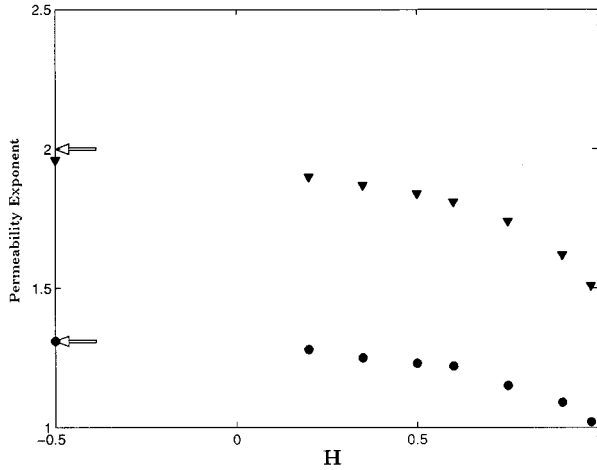
FIG. 15. The dependence of the permeability exponent e on H in 2D (circles) and 3D (triangles). Arrows indicate the corresponding values for random percolation.

To confirm that the exponent e and the other percolation exponents discussed below do actually depend on H, and their apparent dependence on H is not the result of a crossover between two limiting cases, we carried out a careful analysis of our permeability data. First, we changed the range $\Delta p = p - p_c$ in which the permeability data were fitted to Eq. (1). We found that, provided that Δp is sufficiently small (roughly speaking, if $\Delta p < 1/Z$, where Z is the coordination number of the network), the exponent e is insensitive to the range of Δp in which the fitting was done, as it must be. Secondly, similar to finite-size scaling, there may be significant correction-to-scaling terms to the power-law dependence of K on Δp, and instead of Eq. (1) one should write $K \sim (p - p_c)^e [b_1 + b_2 (p - p_c)^{-e_1} + \cdots]$, where e_1 is a correction-to-scaling exponent, and the b's are constant. Thus we fitted the permeability data for network sizes $L > L_m$ to this equation to see whether e still varies with H. We found that the effect of correction-to-scaling terms is insignificant, and obtained the same values of e as before. Thus we are confident that the H dependence of the exponents that we find is not the result of a crossover effect, lack of precision in our data, or a finite-size effect.

Consider now a possible application of our correlated percolation model. The application we consider is flow through *field-scale* porous media, such as oil reservoirs and aquifers, and estimating their effective permeability. The fact that the permeability distribution and porosity logs of such porous media appear to obey fGn and fBm statistics indicates that flow in such porous media can be reduced to flow through the sample-spanning cluster of the correlated percolation described in this paper. The idea is that [28–31] in a heterogeneous medium with a broad distribution of the permeabilities or flow conductances, a finite volume fraction of the system has a small permeability or hydraulic conductance, whose contribution to the overall permeability or conductivity is very small. Thus one can eliminate such low permeability or conductance regions of the system, i.e., set their permeability or conductance to be zero, in which case one obtains a percolation system with long-range correlations. Although in the original paper of Ambegaokar, Halperin, and Langer [28] it was assumed that the conductances are exponentially

broad, computer simulations of Berman *et al.* [32] indicated that this idea is still very useful even if the conductance distribution is relatively narrow. However, unlike the previous applications of this idea [29–32], which were to porous media with *microscopic* disorder that were reduced to *random* percolation systems with largely universal scaling properties, in the present problem one has a field-scale porous medium with *macroscopic* disorder that, as shown in this paper, is reduced to a percolation system with nonuniversal properties. Recent computer simulations of Moreno and Tsang [33] and Herweijer and Dubrule [34] confirm the applicability of percolation to flow in field-scale porous media with macroscopic disorder. These authors found that, if a 3D porous medium is represented by a cubic tessellation of rectangular blocks whose permeabilities follow a distribution $F(K)$, then the flow paths are along only the regions with large permeabilities. The volume fraction of such regions was found to depend on $F(K)$. This is precisely the essence of the idea developed in [28–31].

We can use this idea and our results in this paper to obtain an estimate of the permeability K of a field-scale porous medium with a permeability distribution $F(K)$. Suppose that K_c is the critical permeability such that all the permeabilities less than K_c are set to be zero and, following [28–31], the permeabilities of the rest of the pore space are assigned the same value K_c. Equation (1) tells that

$$K \sim K_c [p(K) - p(K_c)]^e, \tag{20}$$

where $p(K) = \int_K^\infty F(K) dK$ is the fraction of the regions of the pore space having a permeability larger than K. We need to eliminate $p(K) - p(K_c)$ from Eq. (20), since it cannot be measured directly, and replace it with some measurable quantity. Thus following Refs. [28–31] we maximize Eq. (20) with respect to K_c, which yields $p(K) - p(K_c) = e K_c F(K_c)$, implying that

$$K \sim e^e K_c^{1+e} [F(K_c)]^e. \tag{21}$$

Therefore, given a permeability distribution $F(K)$, we first estimate the exponent e and the percolation threshold p_c, from which the critical permeability K_c is estimated. Then, Eq. (21) provides us with an estimate of the overall permeability K of the pore space. In particular, if the distribution $F(K)$ of the porous medium gives rise to a nonuniversal scaling law for the permeability K, in which the critical exponent e depends on some parameter of the distribution, then the dependence of e on this parameter also has to be determined. If the permeability distribution obeys the statistics of a fBm, then Figs. 7 and 12 give the desired dependence of p_c (and thus K_c) and e on H. Therefore in any practical application one also has to determine H for a given field-scale porous medium. Early analysis of Hewett and Behrens [15,16] had indicated that for many rocks $H > 0.7$. However, more recent and careful studies [17–19,35] suggest that in fact $0 < H < 0.5$.

IV. SUMMARY AND DISCUSSION

Summarizing our results, some of the critical exponents that characterize the scaling properties of our percolation model depend at most weakly on H, the parameter that char-

acterizes the nature of the correlations, while some others depend smoothly and strongly on H. As a result, most scaling properties of this percolation model are *nonuniversal*.

Another possible application of our model is [5] to dispersion in field-scale porous media. Dispersion, the unsteady mixing of two miscible fluids displacing one another in a porous medium, is caused by a chaotic velocity field in the pore space. It can be modified by molecular diffusion which transfers the solute (the displacing agent) out of the stagnant regions of the pore space and the slow boundary layer zones near the pore walls. Dispersion is important to enhanced recovery of oil, salt-water intrusion in coastal aquifers, pollution of groundwater flow, and several other phenomena [2–4]. Dispersion in *homogeneous* porous media is usually modeled by the convective-diffusion equation (CDE),

$$\frac{\partial C}{\partial t} + \mathbf{v} \cdot \boldsymbol{\nabla} C = D_L \frac{\partial^2 C}{\partial x^2} + D_T \nabla_2^2 C, \qquad (22)$$

where C is the solute concentration, $\mathbf{v}$ the average flow velocity, D_L the longitudinal dispersion coefficient (in the direction of macroscopic flow x), and D_T and ∇_2^2 are the dispersion coefficient and the Laplacian in the transverse (perpendicular to the macroscopic flow) directions, respectively. An important characteristic of dispersion is the dispersivity $\alpha_L = D_L/\mathbf{v}$, which is the length scale above which a description of dispersion by a CDE is valid. Description of dispersion by a CDE assumes that $\mathbf{v}$, D_L, D_T, and α_L are independent of length scale and time, and has been reasonably successful for porous media at *small* length scales (of order of at most a few meters) [3,4].

However, there have been several *field* studies of dispersion [36–39] indicating that D_L and α_L are scale and time dependent, $\alpha_L \sim L^\delta$ and $\alpha_L \sim t^\chi$, and that D_L depends linearly on $\mathbf{v}$ and thus on the permeability K. Here L is the length scale of the measurements or the distance from the source (where the solute or the displacing fluid is injected into the flowing fluid in the rock). A nonuniversal $\chi \simeq 0.5$–0.6 has been found [40–42] to provide a reasonable fit of the data. Although various theories have been proposed [40–42], up to now, the anomalous dependence of α_L on L and t has not found a completely satisfactory explanation. However, as discussed above, if the rock permeabilities are distributed according to a fBm, then the pore space in which flow and dispersion take place is similar to the sample-spanning cluster of the correlated percolation system studied here [43,44]. It is then not difficult to show that [5,45]

$$\alpha_L \sim t^{1/(1+\theta)}, \qquad (23)$$

where $\theta = (e - \beta_B)/\nu$, which means that $\chi = 1/(1+\theta)$, and thus χ is related to the critical exponents of our model.

We argue that it is the *two-dimensional* correlated percolation that is relevant to the interpretation of the field-scale dispersion data, since such data are obtained at large distances from the source (up to several tens of kilometers), whereas the thickness of such porous media is at most a few hundred meters, and therefore such porous media are long and thin, and thus essentially two dimensional. Therefore one has to use the critical exponents of our 2D percolation with long-range correlations to estimate θ and hence χ. Our results in this paper indicate that these exponents are nonuniversal, consistent with the field data that indicate that χ is nonuniversal and varies from field to field. In fact, using our results we estimate that $\chi \simeq 0.5$–0.60 for $0 < H < 1$, consistent with the range of experimental data discussed above. We thus propose that percolation with long-range correlations is relevant to dispersion phenomena in field-scale porous media and aquifers, and provides a rational and plausible explanation for the nonuniversality of the dispersivity exponent χ, and how it may depend on the structure of the field-scale porous media (i.e., on the value of H that characterizes the nature of the correlations).

Another possible application of our percolation model is to modeling the fracture network of heterogeneous rock. The analysis of fracture surfaces and 3D fracture networks of rock masses at large scales [46] indicates that the fracture networks may have the structure of a percolation cluster. Moreover, similar to our correlated percolation model, the fracture networks of rock are dense, confirming the existence of long-range correlations in the rock. We plan to explore this possibility in future work.

These are just a few possible applications of our percolation model with long-range correlations to some practical problems. We hope that this paper will stimulate more work in this interesting and, from a practical viewpoint, important area.

[1] D. Stauffer and A. Aharony, *Introduction to Percolation Theory*, 2nd ed. (Taylor and Francis, London, 1994).

[2] M. Sahimi, *Applications of Percolation Theory* (Taylor and Francis, London, 1994).

[3] M. Sahimi, Rev. Mod. Phys. **65**, 1395 (1993).

[4] M. Sahimi, *Flow and Transport in Porous Media and Fractured Rock* (VCH, Weinheim, 1995).

[5] M. Sahimi, J. Phys. France I **4**, 1263 (1994).

[6] A. Coniglio, C. Nappi, L. Russo, and F. Peruggi, J. Phys. A **10**, 205 (1977).

[7] A. Weinrib and B. I. Halperin, Phys. Rev. B **27**, 413 (1983).

[8] A. Weinrib, Phys. Rev. B **29**, 387 (1984).

[9] M. B. Isichenko and J. Kalda, J. Nonlinear Sci. **1**, 255 (1991).

[10] S. Prakash, S. Havlin, M. Schwartz, and H. E. Stanley, Phys. Rev. A **46**, R1724 (1992).

[11] J. Schmittbuhl, J.-P. Vilotte, and S. Roux, J. Phys. A **26**, 6115 (1994).

[12] B. B. Mandelbrot and J. W. Van Ness, SIAM Rev. **10**, 422 (1968).

[13] S. Rambaldi and O. Pinazza, Physica A **208**, 21 (1994).

[14] H. H. Hardy and R. A. Beier, *Fractals in Reservoir Engineering* (World Scientific, Singapore, 1994).

[15] T. A. Hewett, Society of Petroleum Engineers, Report No. 15386, 1986 (unpublished).

[16] T. A. Hewett and R. A. Behrens, SPE Form. Eval. **5**, 217 (1990).

[17] H. Rassamdana, A. R. Mehrabi, and M. Sahimi (unpublished).

[18] M. Sahimi, H. Rassamandana, and A. R. Mehrabi, in *Fractal Aspects of Materials*, edited by Fereydoon Family *et al.*, MR/S Symposia Proceedings No. 367 (Materials Research Society, Pittsburgh, 1995), p. 203.

[19] A. R. Mehrabi, H. Rassamdana, and M. Sahimi (unpublished).

[20] S. P. Neuman, Water Resour. Res. **31**, 1455 (1995).

[21] E. L. Hinrichsen, A. Aharony, J. Feder, A. Hansen, T. Jøssang, and H. H. Hardy, Transport Porous Media **12**, 55 (1993).

[22] M. Sahimi, G. R. Gavalas, and T. T. Tsotsis, Chem. Eng. Sci. **45**, 1443 (1990).

[23] M. E. Fisher, in *Critical Phenomena*, Proceedings of the International School of Physics ''Enrico Fermi,'' edited by M. S. Green (Academic, New York, 1971), p. 1.

[24] M. Levinshtein, M. S. Shur, and E. L. Efros, Zh. Eksp. Teor. Fiz. Sov. Phys. JETP **42**, 1120 (1976).

[25] P. J. Reynolds, H. E. Stanley, and W. Klein, Phys. Rev. B **21**, 1223 (1980).

[26] M. D. Rintoul and H. Nakanishi, J. Phys. A **25**, L945 (1992).

[27] B. I. Halperin, S. Feng, and P. N. Sen, Phys. Rev. Lett. **54**, 2891 (1985).

[28] V. Ambegaokar, B. I. Halperin, and J. S. Langer, Phys. Rev. B **4**, 2612 (1971).

[29] V. K. S. Shante, Phys. Rev. B **16**, 2597 (1977); S. Kirkpatrick, in *Ill-Condensed Matter*, edited by R. Balian, R. Maynard, and G. Toulouse (North-Holland, Amsterdam, 1979), p. 323.

[30] A. J. Katz and A. H. Thompson, Phys. Rev. B **34**, 8179 (1986).

[31] M. Sahimi, AIChE J. **39**, 369 (1993).

[32] D. Berman, B. G. Orr, H. M. Jaeger, and A. M. Goldman, Phys. Rev. B **33**, 4301 (1986).

[33] L. Moreno and C. F. Tsang, Water Resour. Res. **30**, 1421 (1994).

[34] J. C. Herweijer and O. R. F. Dubrule, J. Pet. Technol. **47**, 973 (1995).

[35] S. Painter and L. Paterson, Geophys. Res. Lett. **21**, 2857 (1994).

[36] A. Arya, T. A. Hewett, R. G. Larson, and L. W. Lake, SPE Reservoir Eng. **3**, 139 (1988).

[37] J. F. Pickens and G. E. Grisak, Water Resour. Res. **17**, 1191 (1981).

[38] F. J. Molz, O. Güven, and J. G. Melville, Ground Water **21**, 715 (1983).

[39] E. A. Sudicky, J. A. Cherry, and E. O. Frind, Water Resour. Res. **21**, 1035 (1985).

[40] S. P. Neuman, Water Resour. Res. **26**, 887 (1990).

[41] R. Ababou and L. W. Gelhar, in *Dynamics of Fluids in Hierarchical Porous Media*, edited by J. H. Cushman (Academic, London, 1990), p. 393.

[42] J. R. Philip, Transport Porous Media **1**, 319 (1986).

[43] P. G. Saffman, J. Fluid. Mech. **6**, 321 (1959).

[44] D. L. Koch and J. F. Brady, J. Fluid. Mech. **154**, 399 (1985).

[45] M. Sahimi, J. Phys. A **20**, L1293 (1987); M. Sahimi and A. O. Imdakm, *ibid.* **21**, 3833 (1988).

[46] M. Sahimi, M. C. Robertson, and C. G. Sammis, Phys. Rev. Lett. **70**, 2186 (1993); M. C. Robertson, C. G. Sammis, M. Sahimi, and A. J. Martin, J. Geophys. Res. **100B**, 609 (1995).